DETERMINATION OF TRACE SILICONE CONTAMINATION ON COMPOSITES BY QUANTITATIVE XPS AND LIBS

Rodolfo Ledesma[1], Giles Dillingham[2], Brooke Campbell[2], Frank Palmieri[3], William Yost[3], Yi Lin[4], James Fitz-Gerald[1], and John Connell[3]

1. University of Virginia, Charlottesville, VA 22904 USA
2. BTG Labs, Cincinnati, OH, 45217 USA
3. NASA Langley Research Center, Hampton, VA 23681 USA
4. National Institute of Aerospace, Hampton, VA 23666 USA

ABSTRACT

Surface treatment and surface characterization techniques are critical to ensure that adherends are chemically activated and free of contaminants prior to adhesive bonding. Silicone contamination from mold-release agents and other sources can interfere with interfacial bonding, decreasing the durability and performance of bonded composite structures. Tools and methods are needed that can be used in a production environment to reliably detect low levels of contaminants in a rapid, simple, and cost-effective manner to improve bond reliability. In this work, surface characterization of carbon fiber reinforced polymer (CFRP) composites was performed using laser induced breakdown spectroscopy (LIBS) and the results were compared with those obtained from X-ray photoelectron spectroscopy (XPS). The objective was to investigate the ability to quantify the surface species measured by LIBS since it offers many advantages over XPS in terms of ease of use, sample preparation, and real-time results. The as-processed CFRP panels had trace surface silicone contamination from the fabrication process, the source of which was not investigated. The composites were laser treated at select average laser power levels, resulting in varying levels of contamination reduction. The Si atomic percentage measurements using XPS were conducted both before and after laser ablation. The XPS results were compared with those obtained from LIBS to assess the reliability of each technique for surface contaminant characterization. The results showed an excellent correlation in Si atomic concentration between the two techniques.

1. INTRODUCTION

The use of adhesive bonding in aerospace structures has many advantages over traditionally fastened components in terms of simplification in manufacturing and structural performance. However, before this approach can be used on primary structures in commercial aircraft, a number of issues must be addressed [1]. The Federal Aviation Administration (FAA) has established certification criteria for adhesively bonded aircraft components. Currently, secondary structural components can rely on adhesive bonding for structural performance without any requirements for secondary arrest features or mechanical fasteners. However, primary adhesively bonded aircraft structures require secondary arrest features in most cases [2]. Adhesive bonding has been highly successful for secondary structural applications, but when failures occurs, they are often traced back to poor or incomplete surface preparation, surface contamination, or related issues. Thus, the guidelines provided by the FAA also focus on process control and verification methods of surface readiness for adhesive bonding. A major goal of the NASA Advanced Composite Project (ACP) is reducing the timeline to certification by 30% for composite structures on commercial transport

aircraft. Within the Efficient Manufacturing Processes Technical Challenge under ACP, there is a task focused on bonded structure and automated surface treatment. Within this task, team members from The Boeing Company, United Technologies-Pratt and Whitney, UTC Aerospace Systems and NASA Langley Research Center (LaRC) have been evaluating various surface treatment methods, effects of various contaminants on adhesive bonding, and characterization tools for surface analysis [3-7]. The use of laser ablation has been shown to be an attractive means of surface preparation of CFRP composites and metal alloys by providing a clean, high precision, reproducible surface that provides high quality adhesive bonds [8-12]. As part of this work, a tool was developed utilizing laser induced breakdown spectroscopy (LIBS) for rapid determination of low levels of problematic contaminants [13]. Prior work has identified silicones as significant threats to adhesive bonding even at exceptionally low concentrations (~0.8 μg/cm^2). The ability of commercial off-the-shelf (COTS) tools to reliably detect such low concentrations of silicones on surfaces was found to be lacking in requisite sensitivity and precision, ease of use, and/or data acquisition and analysis time. In some cases, COTS tools require destructive, time consuming sample preparation methods. In contrast, LIBS, in conjunction with laser ablation surface treatment, has shown significant promise in detecting silicones at concentrations well below the level known to be a threat to bonding. In this work, the sensitivity of LIBS in detecting silicones was compared with that of X-ray photoelectron spectroscopy (XPS). Unlike XPS, LIBS analysis is conducted in the open air, no sample preparation is necessary, and the results are nearly instantaneous. The work described here involved fabrication of two-ply composite laminates which had inherent silicone contamination, followed by LIBS analysis and XPS analysis. The results show an excellent correlation between the silicone levels detected by LIBS and XPS.

1.1 Laser Surface Treatment

Laser surface treatment enables high precision processing that lends itself to automation and reproducibility for surface activation and removal of surface contaminants on CFRP surfaces [3-16]. By adjusting the laser parameters, it is possible to control the laser-solid interactions to remove surface contaminants and induce texture to the surface without exposing or damaging the carbon fibers underneath the resin surface layer. This technique can also be used for other surfaces such as metal alloys, and can be used to selectively remove surface layers such as paint or coatings without affecting the underlying substrate.

In this work, a picosecond laser was used to chemically activate and remove surface contaminants (e.g. silicones) on CFRP surfaces. Picosecond and ultrashort laser pulses ablate the polymer surface material by multiphoton absorption, inducing photochemical ablation [17-21]. The rapid ejection of the laser-excited material from the solid reduces the heat transfer to the substrate outside the excited volume, producing minimal thermal damage [18,21-24]. For the case of CFRP composites, picosecond and ultrashort pulses enable the ablation with low average laser power, which mitigates subsurface interlaminar damage.

1.2 Laser Induced Breakdown Spectroscopy

LIBS is a surface characterization technique that provides chemical information by the analysis of atomic emission lines. The plasma plume induced during ablation emits photons that are characteristic to the ablated material in the plume. In this work, laser pulse energies below 100 μJ were used for LIBS surface analysis, referred to as μLIBS [13,25-29]. The laser system used for laser surface treatment was the same as that for LIBS surface characterization, providing the

opportunity for in-situ surface inspection prior to and after laser ablation. The implemented LIBS system in the LaRC laboratory enabled the non-destructive surface characterization of CFRP surfaces in a rapid manner without any sample preparation or special atmospheric conditions [13].

1.3 X-ray Photoelectron Spectroscopy

XPS is a quantitative surface characterization technique that provides chemical information about a material, including the elemental composition at the parts per thousand range, empirical formula, chemical state, and electronic state, with a typical depth sensitivity between 10 Å and 50 Å. By irradiating the material with an X-ray source, the kinetic energy of the ejected electrons is measured. The take-off angle can influence the detected electron flux and therefore, the surface sensitivity. To enable high surface sensitivity, the instrument's analysis chamber must be maintained at high vacuum (HV) or ultra-high vacuum (UHV), typically between 10^{-7} and 10^{-10} Torr. This required vacuum level limits the sample chamber size, which necessitates substantial composite specimen dimensional preparation. Following data collection, a significant amount of data reduction must be conducted to extract the desired information concerning the chemical composition of surface species.

2. EXPERIMENTATION

2.1 Materials

The experimental methods and materials have been described previously [12,13]. Unidirectional CFRP panels (30.5 cm × 30.5 cm) were fabricated from two plies of unidirectional Torayca P2302-19 (T800H/3900-2) prepreg. The curing process was performed in an autoclave at 177 °C and 690 kPa. Release of the composite panel from the caul plate was achieved using Airtech A4000V release film, a fluorinated ethylene propylene (FEP) film. Tool and caul surfaces were pre-treated with Zyvax WaterShield, a silicone-based mold release agent dispersed in water. CFRP coupons of 2 cm × 3 cm were prepared for LIBS surface characterization. Subsequently, for XPS analysis, those coupons were cut with scissors into four specimens of 1 cm × 1.5 cm.

2.2 Laser Ablation

Laser ablation was performed with a Nd:YVO_4 (Atlantic 20-355, EKSPLA) laser operated at 355 nm and ~10 ps pulse width. To produce different surface conditions, two-ply unidirectional CFRP surfaces were laser processed using a pulse frequency of 400 kHz at select average laser power levels, ranging from 40 mW to 180 mW. The average laser power was measured with a thermopile sensor (30A-BB-18, Ophir-Spiricon) and a laser power meter (Nova II, Ophir-Spiricon). The CFRP surfaces were laser ablated with parallel lines, which were produced in the fiber direction at 12.7 μm line pitch and 25.4 cm/s scan speed. These laser conditions were constant throughout all of the experiments except for the laser power.

2.3 Laser Induced Breakdown Spectroscopy

The laser system utilized for LIBS characterization experiments was the same that was used for laser ablation surface treatment. The laser pulse energy was 15 μJ (7.53 J/cm^2). The LIBS emission was collected using a 328 mm, f/4.6 Schmidt-Czerny-Turner (SCT) spectrograph (IsoPlane SCT 320, Princeton Instruments). The spectral response was recorded using an electron-multiplier intensified charge-coupled device (emICCD) camera (PI-MAX4: 1024 EMB, Princeton

Instruments), which was externally triggered by the laser trigger output. The plasma emission was collected with a collimator and guided to the spectrograph via an optical cable with 19 fibers (200 μm each). A grating with 600 grooves/mm, blazed at 300 nm, and a slit width of 10 μm were used. A LIBS spectrum was generated by averaging 10 frames of 10 single laser shots. The target surface was moved with a XY stage after each single shot to expose a fresh surface for each incident pulse. The 10 single laser shots were accumulated on the CCD sensor.

2.4 X-ray Photoelectron Spectroscopy

XPS analysis was performed in two separate facilities, one in the LaRC laboratory (Hampton, VA) and the other in BTG Labs (Cincinnati, OH). In the LaRC laboratory, the CFRP coupons, 1 cm × 1.5 cm, were characterized with a DESA-100 analyzer (STAIB Instruments) and a monochromatic Al K-alpha X-ray (1.486 keV photon energy) source, operated at 15 kV. Three survey scans were performed from 1100 eV to 0 eV on the CFRP surface. Each survey scan was taken in a different location on the sample surface. The take-off angle was 90°.

In BTG Labs, the CFRP coupons were analyzed with a Surface Science Instruments SSX-100 and a monochromatic Al K-alpha X-ray (1.486 keV photon energy) source, operated at 10 kV. The analysis area was 800 μm × 800 μm, and the take-off angle was 45°. Each survey scan was taken in a different location on the target surface.

2.5 Scanning Electron Microscopy

Two-ply CFRP surfaces were coated with Pd-Au for scanning electron microscopy (SEM) measurements and analyzed using a JEOL JSM-5600 scanning electron microscope operated at an accelerating voltage of 15 kV. High resolution SEM (HRSEM) measurements were conducted on a Hitachi S-5200 field emission scanning electron microscope operated at 20 kV.

3. RESULTS AND DISCUSSION

The CFRP surfaces were laser ablated at select laser power levels to produce various surface conditions. The same surface conditions were analyzed by XPS and the results were correlated to the Si/C ratio from LIBS. In the LIBS experiments, the C and Si emission lines at 247.9 nm and 288.2 nm were used in the analysis. Concerning XPS, Si species were measured by looking at the electron binding energies of specific electrons. In addition, the silicone removal efficiency of the laser surface ablation was evaluated by adjusting the laser power and correlating it to the Si/C ratio. Modification of the surface topography after laser ablation was analyzed by SEM.

The laser power conditions for treatment of the two-ply unidirectional CFRP surfaces are shown in Table 1. By changing the laser power, the amount of silicone contaminant removed was varied. For LIBS experiments, 20 measurements were conducted at different locations on the CFRP coupon of 2 cm × 3 cm. The same coupons were cut into four coupons of 1 cm × 1.5 cm. For the measurements at LaRC, one coupon was analyzed, while BTG Labs analyzed two coupons. Regarding the CFRP surfaces ablated at 120 mW, two coupons were inspected at LaRC and four at BTG Labs. Several aspects of XPS analyses at the two facilities were different. The take-off angles for the two instruments (LaRC, 90°), and (BTG, 45°), can affect the results, especially at high silicone concentrations. The time that elapsed after laser ablation treatment and when the XPS analyses were performed was also different. Typically, at LaRC, the XPS analysis were conducted

within 24 to 48 hours after laser treatment since the laser system and XPS instrument were co-located. In the case of BTG, more time elapsed (72 to 96 hours) between the laser treatment and XPS analyses since the samples had to be packaged and shipped after laser treatment at LaRC.

Table 1. Summary of experimental conditions of XPS analysis.

Laser power (mW)	Number of Measurements	
	LaRC	BTG Labs
0 (Control)	3	4
40	3	4
60	3	6
80	3	6
90	3	6
100	3	4
120	6	12
140	3	6
160	3	6
180	3	6

3.1 Surface Characterization Analysis

Figure 1 shows the Si/C ratio from the LIBS results as a function of the Si concentration determined by XPS. In LIBS, the Si emission lines detected were assumed to emanate from the Si in the polymeric silicone contaminant. The Si/C ratio was determined from the Si I emission line at 288.2 nm and the C peak at 247.9 nm. It is assumed that all Si species detected by XPS emanated from the polysilicone contaminant. The Si 2p peak was chosen for the detection and measurement of trace silicone on CFRP surfaces. Linear fit equations were applied to each XPS data set. The y-intercepts of the linear fits were zero and both slopes were similar. At higher concentrations, the difference between XPS measurements (LaRC and BTG) was ~1 at.%, and at lower concentrations the measurements converged. The difference in take-off angles may influence that result, since they can affect the concentration of Si with respect to other elements due to differences in sample interrogation depth. Overall, the XPS results showed excellent agreement in silicon content, suggesting that the difference in time elapsed between laser treatment and XPS analysis (within the time frame mentioned) did not affect the silicone surface contamination. Also, the chart shows that increasing laser power led to more efficient removal of silicone contaminant. In previous work from our laboratory, Si/C ratios of less than 0.2 resulted in high quality bonded specimens that failed ~100% cohesively.

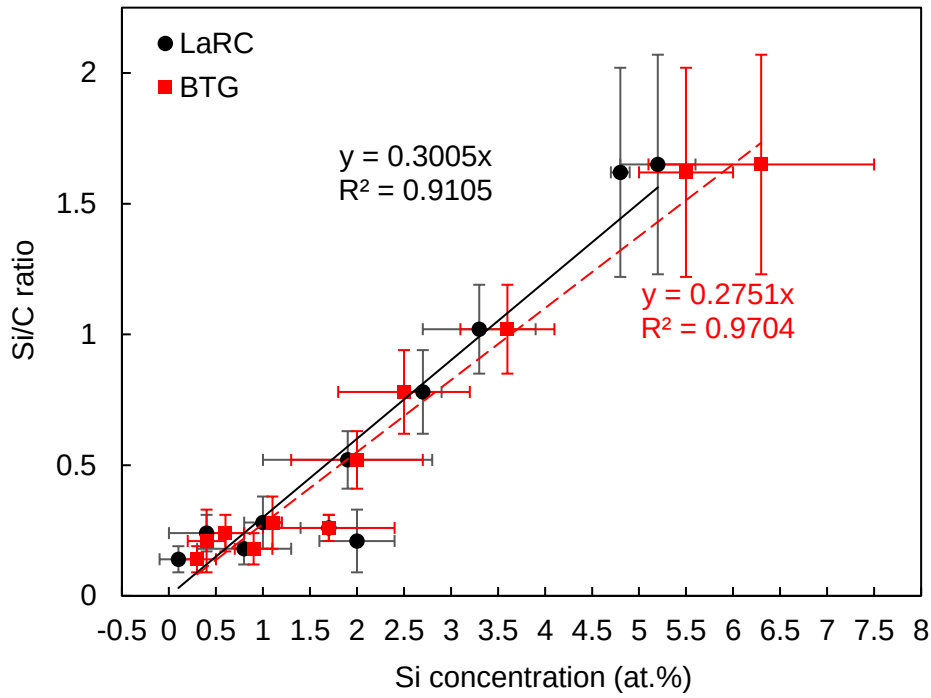

Figure 1. Si/C from the LIBS measurements as a function of Si concentration measured by XPS from both NASA LaRC and BTG Labs.

The Si/C ratios determined from LIBS and XPS are compared in Figure 2. The slopes of the linear fits were similar with both y-intercepts set to zero. This again shows that there was excellent agreement between the two laboratories with respect to the XPS measurements, and a high degree of correlation between the Si/C ratios determined by LIBS and XPS.

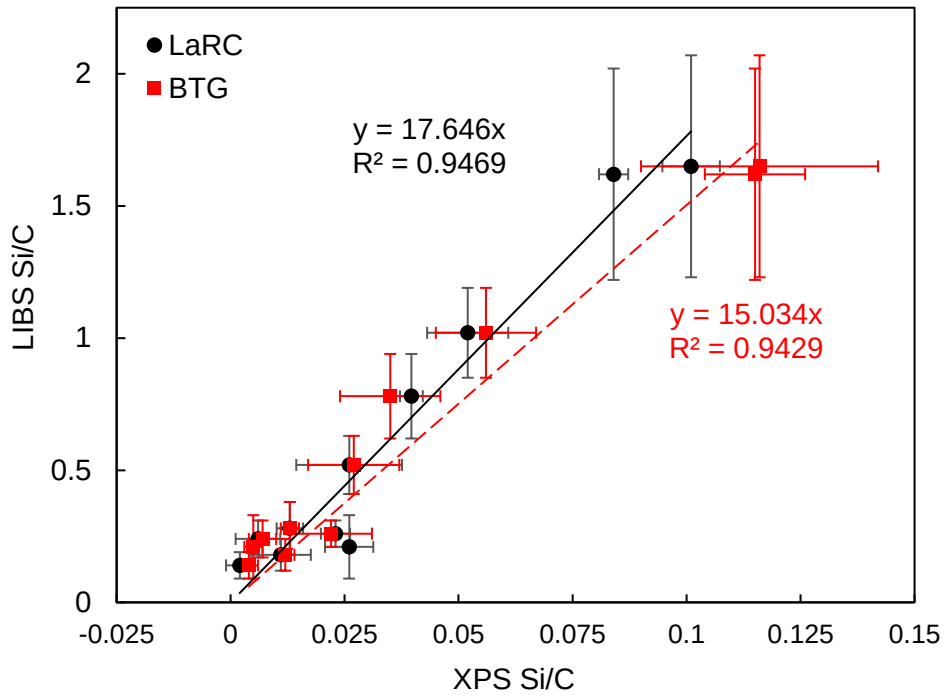

Figure 2. Comparison of LIBS Si/C and XPS Si/C.

The XPS measurements from LaRC and BTG Labs were compared for agreement using the line of equality analysis method, as shown in Figure 3. Each data point represents the mean of the XPS measurements. For Si concentrations below 4 at.%, the data points were closer to the line of equality. Above 4 at.%, there was some difference, likely due to the difference in take-off angles of the two instruments used. Also, there was a data point that seems statistically inconsistent with the rest of the data. A possible explanation was that silicone was not removed as efficiently as in the surrounding regions (the coupons sent to BTG yielded low Si atomic percentage, which agrees well with the low Si/C ratio). Another reason could be that the specific region interrogated had an unusually high amount of silicone compared to the surrounding regions. No outlier analysis was performed, and consequently, no outliers were rejected from the reported data.

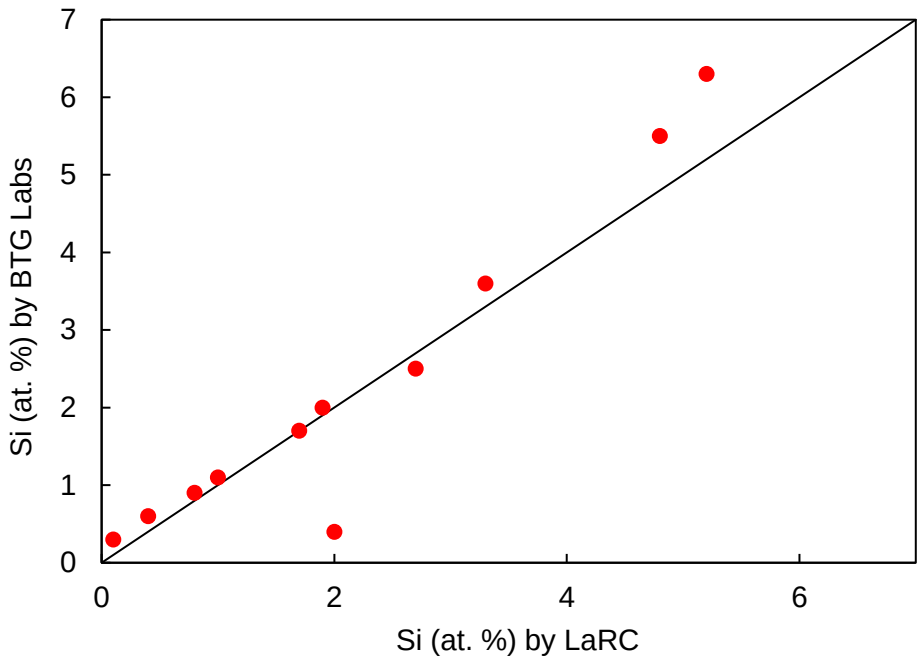

Figure 3. Mean Si concentration measured by XPS from LaRC and BTG Labs, with line of equality.

3.2 Laser Ablation Performance

The laser ablation performance was studied using the Si/C ratio from the LIBS measurements. The laser ablation at different laser power levels produced different surface conditions and thus different Si/C ratios. Figure 4 shows the Si/C ratio as a function of the average laser power. Each data point was the average of 20 measurements, except for the data point at 120 mW, which was the average of 40 measurements. At 40 mW, the UV laser pulses did not produce measurable surface modification on the two-ply unidirectional CFRP surface. This was likely due to the laser power being below the ablation threshold of the epoxy matrix. This can be seen clearly in the SEM micrograph in Figure 5(a), where the CFRP surface remained almost intact after 40 mW laser treatment. Therefore, the Si/C ratios of the control surface (0 mW laser power) and the surface ablated at 40 mW were similar since no significant ablation occurred. As an optical material, silicone weakly absorbs from the UV to visible wavelengths (200 nm to 750 nm) [30]. However, the resin surface layer in CFRP has higher absorption levels at 355 nm [14,31,32]. Thus, the removal of silicone contamination in CFRP composites was coupled with preferential ablation of the epoxy resin. As mentioned previously, it was empirically determined that Si/C ratios below 0.2 gave good adhesive bonds (~100% cohesive failure) with this composite system and EA9696 epoxy film adhesive. This means that the desired laser power under the previously described scan speed, frequency, and pitch, should be at least 100 mW. However, it is important to know how much silicone contamination is on the CFRP surface prior to laser ablation surface treatment so that ablation parameters can be judiciously selected.

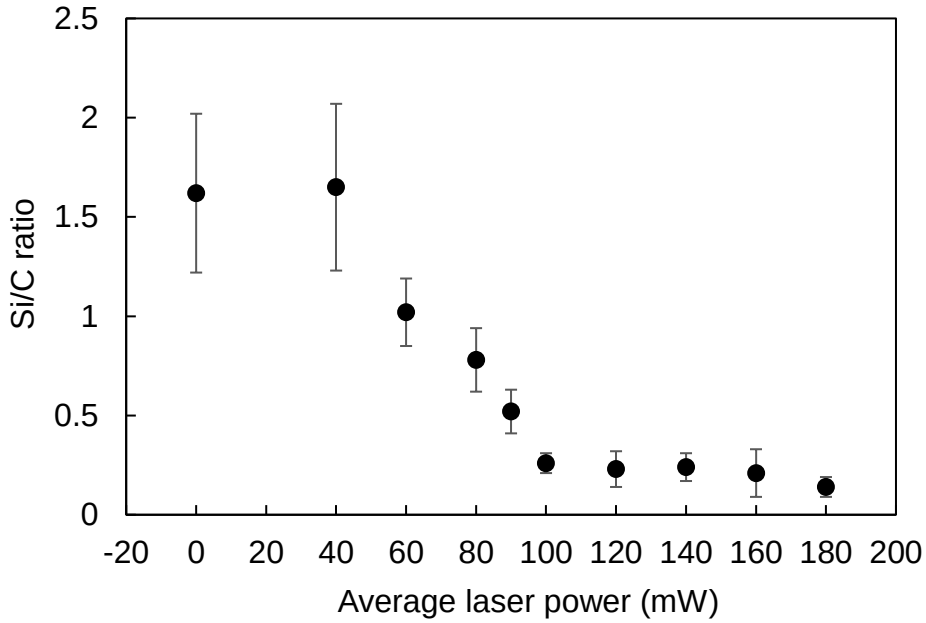

Figure 4. Si/C from LIBS as a function of average laser power. The laser power of zero corresponds to the control surface.

At a minimum, micro- and nanoscale roughness increases the interfacial surface area which can lead to mechanical interlocking, improving bond performance. Figure 5 shows the SEM micrographs of the laser ablated CFRP surfaces for select laser power levels. Again, there was no substantial surface modification in some regions by the 40 mW picosecond laser pulses. Whereas on some edges, as shown in Figure 5(a), the ablative lines were more evident. As the power increased, the laser ablation was more significant and sufficient to remove the resin surface layer, as shown in Figures 5(b) to 5(d). The SEM micrographs also show that the resin surface layer was removed without exposing the underlying carbon fibers. No exposure of carbon fibers or heat affected zones were observed. The resin surface layer thickness was non-uniform and after laser ablation, there were some locations that showed clusters of epoxy resin while other treated locations resulted in a smoother resin surface.

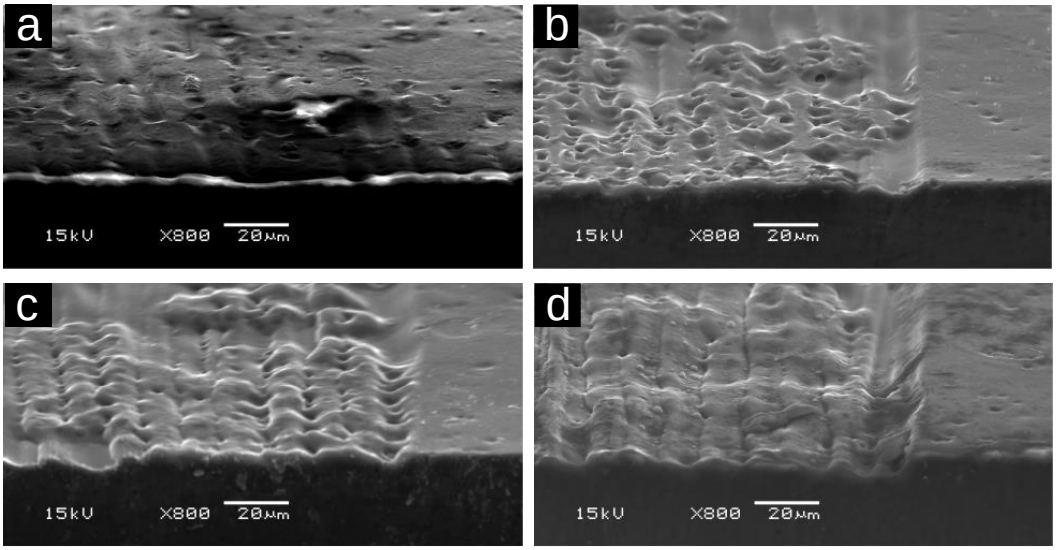

Figure 5. SEM micrographs of laser ablated CFRP surfaces at average laser power levels of a) 40 mW, b) 80 mW, c) 120 mW, and d) 180 mW. There is no exposure of underlying carbon fibers.

Figure 6 shows the HRSEM micrographs for the selected CFRP surfaces consisting of the control 6(a), and ablated at 80 mW 6(b), 120 mW 6(c), and 180 mW 6(d). The control surface did not show any significant features. In contrast, the surfaces ablated at 80 mW, 120 mW, and 180 mW power levels appeared to have particulates that were between 100 nm to 300 nm in diameter. The surface ablated at 80 mW showed a flattened pattern of those nanostructures, in contrast, the surface ablated at 180 mW showed that the nanostructures were standing out of the polymeric surface. It is unclear if these particles are formed as a result of the laser ablation process or if they were present in the matrix resin, perhaps as second-phase toughenners, or a combination of both. The nanoparticles that appeared on the surface are indicative of an inhomogeneity in the surface resin. Energy-dispersive X-ray spectroscopy (EDS) measurements were conducted and no distinct sulfur domains were found. This is likely due to the fact that the curing agent is diaminodiphenyl sulfone (DDS), therefore sulfur is ubiquitously present on the surface. Since the chemical composition of the epoxy resin is not publicly disclosed, the precise composition of the particles cannot be discussed. Further work is underway to determine the source of the nanoparticles.

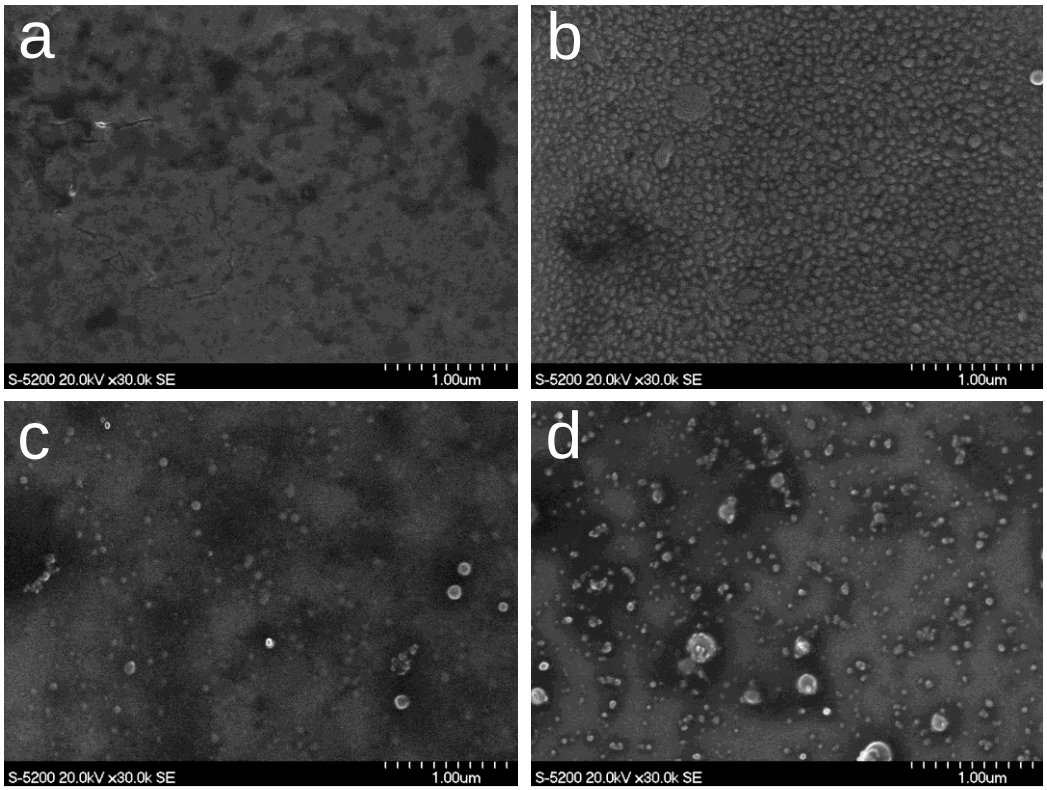

Figure 6. HRSEM micrographs of a) control CFRP, and CFRP surfaces ablated at average laser power levels of b) 80 mW, c) 120 mW, and d) 180 mW.

4. CONCLUSIONS

LIBS analysis of silicone surface contamination was conducted using a picosecond laser on control and laser surface treated CFRP surfaces. The Si/C ratio from LIBS was compared with the Si concentration (Si 2p) from quantitative XPS using two different instruments. With the LIBS system developed at LaRC, Si concentrations below 0.5 at.% were detected on CFRP surfaces. In addition, the XPS results from both measurement systems, LaRC and BTG Labs, showed good agreement by analysis of the line of equality. These results validate the XPS data from LaRC in comparison with the established XPS system from BTG Labs. The agreement and correlation of the XPS results are good despite some differences in the measurement parameters, e.g. the take-off angle, and time elapsed after laser surface treatment. The correlation between the Si/C ratios determined by LIBS exhibited excellent correlation with those determined by XPS. These results demonstrate the ability of LIBS to be used as a high-fidelity tool to detect and measure surface silicone contamination in near real-time with a sensitivity equivalent to XPS.

5. ACKNOWLEDGEMENTS

This work was supported by the NASA Advanced Composites Project. The authors thank Hoa Luong for fabrication of the CFRP panels and John Hopkins for conducting the laser ablation surface treatment.

6. REFERENCES

1. R. Bossi, M. Piehl, “Bonding Primary Aircraft Structure: The Issues”, Manuf. Eng. 146(3) (2011) 101-109.
2. Federal Aviation Administration, Advisory Circular AC 20-107B, Composite Aircraft Structure, 2010.
3. F. Palmieri, M. Belcher, C. Wohl, K. Blohowiak, J. Connell, “Laser Ablation Surface Preparation of Carbon Fiber Reinforced Epoxy Composites for Adhesive Bonding”, SAMPE Electronic Conference Proceedings, 2013.
4. F. Palmieri, R. Ledesma, D. Cataldo, N. Budwal, J. Dennie, Y. Lin, J. Hopkins, C. Wohl, J. Connell, “Laser Ablation to Remove and Detect Silicone Contaminants on Epoxy Matrix Composite”, SAMPE Spring Electronic Proceedings, 2016.
5. E. Kutscha, P. Vahey, M. Belcher, P. VanVoast, W. Grace, K. Blohowiak, F. Palmieri, J. Connell, “Detection of Contamination and Surface Preparation Effects on Bonding of Aerospace Structural Composites”, Adhesion Society Electronic Proceedings, 2017.
6. X. Fang, J. Jalowka, J. Riehl, W. Zhao, D. Goberman, “Contamination Effect on Composite-to-Metal Adhesive Bond Performance”, SAMPE Spring Electronic Proceedings, 2017.
7. E. Kutscha, P. Vahey, M. Belcher, P. VanVoast, W. Grace, K. Blohowiak, F. Palmieri, J. Connell, “Contamination and Surface Preparation Effects on Composite Bonding”, SAMPE Electronic Proceedings, 2017.
8. C. Wohl, M. Belcher, J. Hopkins, J. Connell, “Laser Surface Preparation for Bonding of Aerospace Composites”, Proc. Inst. Civ. Eng.: Eng. Comp. Mech. 164(3) (2011) 133-138.
9. F. Palmieri, K. Watson, G. Morales, T. Williams, R. Hicks, C. Wohl, J. Hopkins, J. Connell, “Laser Ablative Surface Treatment for Enhanced Bonding of Ti-6Al-4V Alloy”, ACS Appl. Mater. Interfaces 5 (2013) 1254-1261.
10. US Patent 8,987,632 B2 “Modification of Surface Energy via Direct Laser Ablative Surface Patterning” March 24, 2015 to NASA.
11. F. Palmieri, M. Belcher, C. Wohl, K. Blohowiak, J. Connell, “Laser Ablation Surface Preparation for Adhesive Bonding of Carbon Fiber Reinforced Epoxy Composites”, Int. J. Adhes. Adhes. 68 (2016) 95-101.
12. F. Palmieri, R. Ledesma, T. Fulton, A. Arthur, K. Eldridge, S. Thibeault, Y. Lin, C. Wohl, J. Connell, “Picosecond Pulsed Laser Ablation for the Surface Preparation of Epoxy Composites”, SAMPE Electronic Proceedings, 2017.
13. R. Ledesma, F. Palmieri, J. Connell, W. Yost, J. Fitz-Gerald, “Surface Characterization of Carbon Fiber Reinforced Polymers by Picosecond Laser Induced Breakdown Spectroscopy”, Spectrochim. Acta, Part B 140 (2017) 5-12.
14. F. Fischer, S. Kreling, P. Jäschke, M. Frauenhofer, D. Kracht, K. Dilger, “Laser Surface Pre-Treatment of CFRP For Adhesive Bonding in Consideration of the Absorption Behaviour”, J. Adhes. 88 (2012) 350-363.
15. F. Fischer, S. Kreling, K. Dilger, “Surface Structuring of CFRP by Using Modern Excimer Laser Sources”, Phys. Procedia 39 (2012) 154-160.

16. F. Fischer, S. Kreling, F. Gaebler, R. Delmdahl, “Using Excimer Lasers to Clean CFRP Prior to Adhesive Bonding”, Reinf. Plast. 57 (2013) 43-46.
17. X. Liu, D. Du, G. Mourou, “Laser Ablation and Micromachining with Ultrashort Laser Pulses”, IEEE J. Quantum Electron. 33 (1997) 1706-1716.
18. M. Shirk, P. Molian, “A Review of Ultrashort Pulsed Laser Ablation of Materials”, J. Laser Appl. 10 (1998) 18-28.
19. E. Campbell, D. Ashkenasi, A. Rosenfeld, “Ultra-Short-Pulse Laser Irradiation and Ablation of Dielectrics”, Mater. Sci. Forum 301 (1999) 123-144.
20. E. Gamaly, A. Rode, V. Tikhonchuk, B. Luther-Davies, “Ablation of Solids by Femtosecond Lasers: Ablation Mechanism and Ablation Thresholds for Metals and Dielectrics”, Phys. Plasmas 9 (2002) 949.
21. J. Krüger, W. Kautek, “Ultrashort Pulse Laser Interaction with Dielectrics and Polymers”, Adv. Polym. Sci. 168 (2004) 247-289.
22. M. Gedvilas, G. Raciukaitis, “Investigation of UV Picosecond Laser Ablation of Polymers”, in: Proc. SPIE, Workshop on Laser Applications in Europe, Vol. 6157, 2005.
23. J. Reif, “Processing with Ultrashort Laser Pulses”, in: P. Schaaf (Ed.), Laser Processing of Materials: Fundamentals, Applications and Developments, Springer, 2010.
24. Z. Cui, “Laser Ablation”, in: D. Li (Ed.), Encyclopedia of Microfluidics and Nanofluidics, Springer, New York, 2014.
25. H. Häkkänen, J. Korppi-Tommola, “UV-Laser Plasma Study of Elemental Distributions of Paper Coatings”, Appl. Spectrosc. 49 (1995) 1721-1728.
26. G. Rieger, M. Taschuk, Y. Tsui, R. Fedosejevs, “Laser-Induced Breakdown Spectroscopy for Microanalysis Using Submillijoule UV Laser Pulses”, Appl. Spectrosc. 56 (2002) 689-698.
27. G. Rieger, M. Taschuk, Y. Tsui, R. Fedosejevs, “Comparative Study of Laser-Induced Plasma Emission from Microjoule Picosecond and Nanosecond KrF-Laser Pulses”, Spectrochim. Acta, Part B 58 (2003) 497-510.
28. I. Gornushkin, K. Amponsah-Manager, B. Smith, N. Omenetto, J. Winefordner, “Microchip Laser-Induced Breakdown Spectroscopy: A Preliminary Feasibility Investigation”, Appl. Spectrosc. 58 (2004) 762-769.
29. I. Cravetchi, M. Taschuk, Y. Tsui, R. Fedosejevs, “Evaluation of Femtosecond LIBS for Spectrochemical Microanalysis of Aluminium Alloys”, Anal. Bioanal. Chem. 385 (2006) 287-294.
30. V.-M. Graubner, R. Jordan, O. Nuyken, T. Lippert, M. Hauer, B. Schnyder, A. Wokaun, “Incubation and Ablation Behavior of Poly(dimethylsiloxane) for 266 nm Irradiation”, Appl. Surf. Sci. 197-198 (2002) 786-790.
31. D. Blass, S. Kreling, S. Nyga, T. Westphalen, B. Jungbluth, H.-D. Hoffmann, K. Dilger, “CFRP Bonding Pre-Treatment with Laser Radiation of 3 μm Wavelength: Laser/Material Interaction”, in: Proc. SPIE, Laser-based Micro- and Nanoprocessing X, Vol. 9736, 2016.
32. K. Takahashi, M. Tsukamoto, S. Masuno, Y. Sato, “Heat Conduction Analysis of Laser CFRP Processing with IR and UV Laser Light”, Composites: Part A 84 (2016) 114-122.